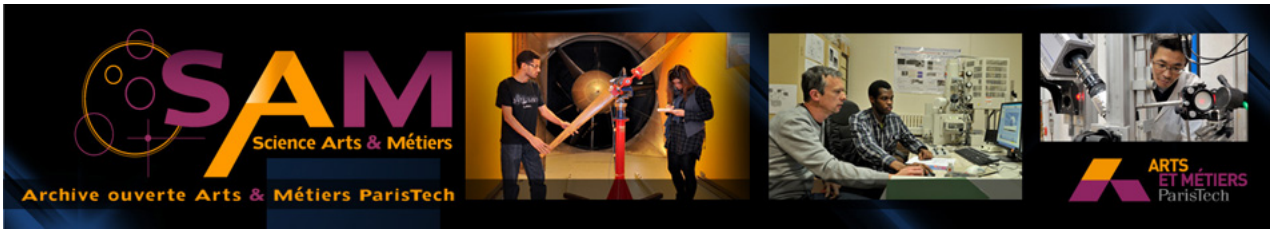

Human Movement Science xxx (2013) xxx–xxx

Contents lists available at ScienceDirect

Human Movement Science

journal homepage: www.elsevier.com/locate/humov

The role of motion platform on postural instability and head vibration exposure at driving simulators

B. Aykent [a,*], F. Merienne [a], D. Paillot [a], A. Kemeny [a,b]

[a] CNRS Le2i Arts et Metiers ParisTech, 2 Rue T. Dumorey, 71100 Chalon sur Saone, France
[b] Technical Centre for Simulation, Renault, Guyancourt, France

ARTICLE INFO

Article history:
Available online xxxx

PsycINFO classification:
2221
2260
4010

Keywords:
Driving simulator
Postural stability
Head vibration exposure

ABSTRACT

This paper explains the effect of a motion platform for driving simulators on postural instability and head vibration exposure. The sensed head level-vehicle (visual cues) level longitudinal and lateral accelerations ($a_{x,\text{sensed}} = a_{x\_\text{head}}$ and $a_{y,\text{sensed}} = a_{y\_\text{head}}$, $a_{yv} = a_{y\_\text{veh}}$ and $a_{yv} = a_{y\_\text{veh}}$) were saved by using a motion tracking sensor and a simulation software respectively. Then, associated vibration dose values (VDVs) were computed at head level during the driving sessions. Furthermore, the postural instabilities of the participants were measured as longitudinal and lateral subject body centre of pressure (X_{CP} and $Y_{CP,}$ respectively) displacements just after each driving session via a balance platform. The results revealed that the optic-head inertial level longitudinal accelerations indicated a negative non-significant correlation ($r = -.203$, $p = .154 > .05$) for the static case, whereas the optic-head inertial longitudinal accelerations depicted a so small negative non-significant correlation ($r = -.066$, $p = .643 > .05$) that can be negligible for the dynamic condition. The X_{CP} for the dynamic case indicated a significant higher value than the static situation ($t(47)$, $p < .0001$). The VDV_x for the dynamic case yielded a significant higher value than the static situation ($U(47)$, $p < .0001$). The optic-head inertial lateral accelerations resulted a negative significant correlation ($r = -.376$, $p = .007 < .05$) for the static platform, whereas the optic-head inertial lateral accelerations showed a positive significant correlation ($r = .418$, $p = .002 < .05$) at dynamic platform condition. The VDV_y for the static case indicated a significant higher value rather than the dynamic situation ($U(47)$, $p < .0001$). The

* Corresponding author. Tel.: +33 (0) 385909865; fax: +33 (0) 385909861.
E-mail address: b.aykent@gmail.com (B. Aykent).

0167-9457/$ - see front matter
http://dx.doi.org/10.1016/j.humov.2013.10.007

Please cite this article in press as: Aykent, B., et al. The role of motion platform on postural instability and head vibration exposure at driving simulators. *Human Movement Science* (2013), http://dx.doi.org/10.1016/j.humov.2013.10.007

Y_{CP} for the static case yielded significantly higher than the dynamic situation ($t(47)$, $p = .001 < 0.05$).

1. Introduction

There are so many implications to be fullfilled in the area of driving simulators. The most important of them is to sustain the reality for the represented dynamics. The major leading problems are the restricted workspace of the driving simulator and whether a motion base exists integrated with the driving simulator. The first driving simulators were fixed-base and the simulation was principally performed by the visual stimulus (Bertin & Berthoz, 2004; Stratulat, Roussarie, Vercher, & Bourdin, 2010) to create the self-motion perception. This perception is based upon the principle of visual scene flow on the retina referring to the velocity, direction of the motion and the relative distances (Bremmer, Kubischik, Pekel, Lappe, & Hoffmann, 1999).

For the static platformed driving simulators, illusory self-motion 'vection' often occurs because the driver is stationary and the visual scenario is mobile (Berthoz, Pavard, & Young, 1975; DiZio & Lackner, 1989; Draper, 1998; Hettinger, 2002; Hettinger, Berbaum, Kennedy, Dunlap, & Nolan, 1990; Hettinger & Riccio, 1992; Kolasinski, 1995; Lepecq et al., 2006; McCauley & Sharkey, 1992).

The incompetencies in the domain of driving simulators, whether they are fixed or motion base simulators, might make the motion sickness an inevitable topic for the development of the researches undertaken.

The methods of evaluating and measuring the motion sickness divesifies depending on the type of the research. In general, there are some ways to assess the sickness level. Some methods refer to the measurements of head level, postural, vehicle and motion platform level dynamics; whereas the verbal methods imply the evaluation via Simulator Sickness Questionnaires (SSQ). Driving simulation sickness was assessed between dynamic and static simulators in some studies (Curry, Artz, Cathey, Grant, & Greenberg, 2002; Watson, 2000). A relation was made between the illness and the head movements of the pilot in absence and presence of the motion base (Kennedy, 1987). A significant reduction in motion sickness occurs when an individual adopts a postural position was expressed in (Reason & Brand, 1975). "Postural instability theory" was introduced also to define relations between perception and the control of action by (Riccio & Stoffregen, 1991). This approach considers the behavior of the individual as fundamental in motion sickness etiology. The postural instability theory of motion sickness presumes that motion sickness is resulted and estimated by instabilities in control of the spine. This was attributed to constraints in motion of the head. Relations were declared between head motions and motion sickness through the mechanisms of Coriolis (with actual inertial cues: motion platform) and pseudo-Coriolis (through visual cues) stimulation (Kennedy et al., 1987; Reason & Brand, 1975). Coriolis stimulation occurs when the head is tilted out of the axis of rotation during actual body rotation (Dichgans & Brandt, 1973; DiZio & Lackner, 1988, 1989; Guedry, 1964; Guedry & Montague, 1961). Pseudo-Coriolis stimulation occurs when the head is tilted as perceived self-rotation that is induced by visual stimuli (Dizio & Lackner, 1989).

In a moving-base simulator, the subjects' head movements were similar to those in the actual vehicle according to those studies in (Dichgans & Brandt, 1973; Dizio & Lackner, 1988, 1989; Guedry, 1964; Guedry & Montague, 1961; Kennedy et al., 1987) where the head movements in fixed-base simulators were often in conflict with the inertial stimulus, which increased the discrepancy of the simulation (Dizio & Lackner, 1989).

Another research on the motion platform effects revealed that using active platform driving simulator yielded more realistic optic-head inertial cues, in other words less conflict, at the lateral dynamics for the passenger condition when the simulator was operated as autopilot mode (Aykent, Merienne, Paillot, & Kemeny, 2013).

Please cite this article in press as: Aykent, B., et al. The role of motion platform on postural instability and head vibration exposure at driving simulators. *Human Movement Science* (2013), http://dx.doi.org/10.1016/j.humov.2013.10.007

Everyday driving experience proposes that drivers are less susceptible to motion sickness than passengers. In the context of inertial motion (i.e., physical displacement), this effect has been confirmed in laboratory research using whole body motion devices. A similar effect was experimented in the context of simulated vehicles in a visual virtual environment. A yoked control design was used in which one member of each pair of participants played a driving video game (i.e., drove a virtual automobile). A recording of that performance was displayed (in a separate session) by the other member of the pair. Thus, the two members of each pair were exposed to identical visual motion stimuli but the risk of behavioral contamination was minimized. Participants who drove the virtual vehicle (drivers) were less likely to report motion sickness than participants who viewed game recordings (passengers). Prior to the onset of subjective symptoms of motion sickness movement differed between participants who (later) reported motion sickness and those who did not, consistent with the postural instability theory of motion sickness. The results verify that control is an important factor in the etiology of motion sickness, and extend this finding to the control of non-inertial virtual vehicles (Dong, Yoshida, & Stoffregen, 2011).

A study has been executed about relations amongst postural instability, motion sickness and vection. 9 males and 4 females (mean age = 19.85 years) were exposed, while standing, to an optical simulation of body sway. Head motion was registered using a motion tracking system. Postural instabilities were monitored prior to the onset of motion sickness. Vection was reported by most participants, including all who became sick. A discriminant analysis indicated that parameters of postural motion accurately predicted motion sickness. The results confirm that postural instability can provoke motion sickness and propose that measures of postural motion may serve as crediable predictors of motion sickness (Smart, Stoffregen, & Bardy, 2002).

Another work has been realized on relations between unstable displacements of the center of pressure and motion sickness. Standing participants were subjected to optic flow in a moving room. Motion sickness was induced by motion that simulated the amplitude and frequency of standing sway. Instabilities were determined in displacements of the center of pressure among participants who became ill; those instabilities occurred before the onset of subjective motion sickness symptoms. Postural differences between 'sick' and 'well' participants were observed before exposure to the nauseogenic stimulus. During exposure to the nauseogenic stimulus, sway increased for participants who became sick but also for those who did not. Nevertheless, at each point during exposure, sway was greater for participants who became motion sick. The results yield that motion sickness is preceded by instabilities in displacements of the center of pressure (Bonnet, Faugloire, Riley, Bardy, & Stoffregen, 2006).

However, there are not so many publications on the subjects' head level vibration exposure and postural instability interactions with the existence and absence of a motion platform (vehicle model: visual longitudinal and lateral acceleration $a_{xv} = a_{x\_veh}$ and $a_{yv} = a_{y\_veh}$ respectively, human head level: longitudinal and lateral acceleration $a_{x\_head} = a_{x,sensed}$ and $a_{y\_head} = a_{y,sensed}$). Because of this fact, the

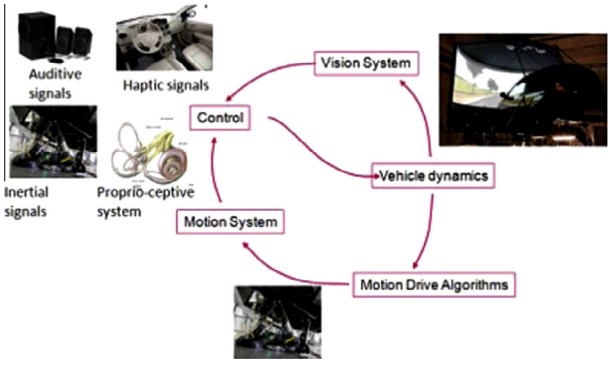

Fig. 1. Structure of the SAAM driving simulator.

Please cite this article in press as: Aykent, B., et al. The role of motion platform on postural instability and head vibration exposure at driving simulators. *Human Movement Science* (2013), http://dx.doi.org/10.1016/j.humov.2013.10.007

participants' head level vibration exposure and postural instability interactions in absence and in presence of the motion platform were surveyed in this article.

This paper also surveys if there is any correlation between the optic-head inertial level accelerations in case of static and dynamic simulators. Optic-head inertial level accelerations stand for the real-time registered and measured visual and vestibular level accelerations. Moreover, the paper tackles how the vestibular level exposed vibration dose values (VDV) differ from each other by activating/deactivating the motion platform of the driving simulator (Fig. 1). Furthermore, this study aims to investigate the motion platform effect on drivers' body centre of pressure (CP) displacement. Finally it tries to find out a relationship between the optic-head inertial acceleration cues correlations with the head level sensed VDV and the bodies' CP displacements of the subjects.

Here, the visual level acceleration refers to the acceleration values registered from the vehicle model that moves in the visual environment for the driving simulator. Whereas the head level acceleration represents the subjects' head accelerations connected to the right ear by using a headphone (Fig. 3) (Aykent et al., 2013).

2. Materials and methods

The research method presented in this study was to compare the motion platform's contribution on postural stability and head level vibration exposures of the subjects.

In order to achieve those objectives, the subjects were asked to drive a specific driving scenario on the simulator.

In the data analysis part, the superposition principle of motion was used for evaluating the sensed longitudinal and lateral dynamics at head level (Fig. 3).

The measured longitudinal acceleration at head level is calculated by Eq. (1) where

$a_{x,\text{sensed}}$: Sensed longitudinal acceleration (m/s^2)
a_{xh}: Longitudinal translational acceleration at head level (m/s^2)
θ: Pitch angle at head level (°)
g: Gravitational acceleration (m/s^2)

$$a_{x,\text{sensed}} = a_{xh} \cdot \cos\theta + g \cdot \sin\theta \tag{1}$$

The measured lateral acceleration in head level is calculated by Eq. (2) where

$a_{y,\text{sensed}}$: Sensed lateral acceleration (m/s^2)
a_{yh}: Lateral translational acceleration at head level (m/s^2)
φ: Roll angle at head level (°)
g: Gravitational acceleration (m/s^2)

$$a_{y,\text{sensed}} = a_{yh} \cdot \cos\varphi + g \cdot \sin\varphi \tag{2}$$

$a_{x,\text{sensed}}$ and $a_{y,\text{sensed}}$ were measured from the participants' right ear levels for the same driven scenario for the static and dynamic platforms via using the sensor in Fig. 3.

In compliance with ISO 2631-1, RMS acceleration values in each axis are defined to more closely reflect the health hazard exposed in the human body. Coefficients are described by ISO 2631-1 on the basis of the frequency and the direction of vibration being exposed to the body. Coefficients of $\omega_k = 0.426$ (cephalocaudal axis) and $\omega_d = 0.067$ (anteroposterior and mediolateral axes) were used to obtain frequency weighted RMS acceleration in each axis (Eqs. (3)–(5)where T is the period of each driving session in seconds). For the evaluation of the health effects, $k_x = 1.4$, $k_y = 1.4$ are chosen. The VDV$_x$ and VDV$_y$ were calculated at "*head*" levels by substituting to the "a_x and a_y" for the head level (Abercromby, Amonette, Layne, et al., 2007; Aykent, Paillot, Merienne, & Kemeny, 2012a; Benson & J., 1988; Griffin, 2004; ISO 2631-1, 1997).

$$VDV = \left[\int_{t=0}^{t=T} a^4(t)dt\right]^{\frac{1}{4}} \tag{3}$$

Please cite this article in press as: Aykent, B., et al. The role of motion platform on postural instability and head vibration exposure at driving simulators. *Human Movement Science* (2013), http://dx.doi.org/10.1016/j.humov.2013.10.007

$$VDV_x = \left[\int_{t=0}^{t=T} (k_x \cdot \omega_k \cdot a_x)^4(t)dt\right]^{\frac{1}{4}} \quad (4)$$

$$VDV_y = \left[\int_{t=0}^{t=T} (k_y \cdot \omega_d \cdot a_y)^4(t)dt\right]^{\frac{1}{4}} \quad (5)$$

2.1. Dynamic driving simulator

The SCANeRstudio and X-Sens measurements are separate measures given as from vehicle level (vehicle model which moves in the visual environment) and as from vestibular level sensed (head dynamics from right ear alignment) respectively. Vehicle level dynamics from the visual environment also affects the head level dynamics. The head dynamics of the drivers are influenced only by the vehicle level dynamics for the static platform case whereas the drivers' head movements are affected by both the vehicle level dynamics and inertial level dynamics (hexapod motion platform) for the dynamic platform condition.

This research work was accomplished under the dynamic as well as static operations of the SAAM (Simulateur Automobile Arts et Métiers) driving simulator (Fig. 1). The dynamic driving simulator SAAM involves a 6 DOF (degree of freedom) motion system (Fig. 1, Tables 1 and 2 (Aykent et al., 2013)). It is exploited on a RENAULT Twingo 2 cabin with the original control instruments (gas, brake pedals, steering wheel). The visual system is realized by a 150° cylindrical view (Fig. 1). With the driving cabin of the simulator, the multi-level measuring techniques are available: vehicle model and motion platform dynamics levels real-time data acquisition via SCANeRstudio driving simulation software, head level dynamics real-time data acquisition via XSens motion tracker, arm and neck muscles dynamics measurement via Biopac EMG (electromyography) device, human's centre of pressure displacements measuring equipment Technoconcept to check postural stability (Aykent et al., 2012a; Aykent, Paillot, Merienne, & Kemeny, 2012b).

Fig. 1 illustrates the SAAM moving-base driving simulator. It could be operated as with static or dynamic platform by switching the "motion platform" module off and on respectively. As seen in the figure, in general there are three dynamical systems of the SAAM driving simulator. They are vehicle dynamics, motion platform dynamics (motion system) and human head dynamics (proprioceptive system). By manipulating or controlling the vehicle dynamics that moves in the vision system and the motion platform dynamics via motion drive algorithms, their effect on human head dynamics can be compared.

In this article, the effect of having an inertial stimulus (motion platform is active and passive separately for the same driving scenario in Fig. 5) on human head dynamics and postural instability were discussed.

$a_{x,\text{sensed}}$ and $a_{y,\text{sensed}}$ were measured to obtain the head level longitudinal and lateral accelerations of the subjects. a_{xh} and a_{yh},which were given in Fig. 2, registered from the vehicle model driven in real-time via the driving simulation software at the same driven scenario for the static and dynamic platforms via using the sensor in Fig. 3.

Fig. 2 describes the motion cueing algorithm used for the dynamic platform case in this research (Aykent et al., 2013). The motion cueing algorithm was included in the SCANeR studio driving simulation software via dll plugin in order to accomplish the real-time driving experiments with the participations of the subjects.

2.2. Head level data acquisition

In order to save the acceleration data from the head level, a motion tracking sensor was used (Fig. 3). The motion tracker can measure the data such as the roll, pitch, yaw angles and rates as well as the accelerations in *X*, *Y* and *Z*. The data are calibrated due to three dimensional quaternion orientation. The sampling rate for the data registration during the sensor measurements was 20 Hz. For the calibrated data acquisition, the alignment reset was chosen which simply combined the object and the

Please cite this article in press as: Aykent, B., et al. The role of motion platform on postural instability and head vibration exposure at driving simulators. *Human Movement Science* (2013), http://dx.doi.org/10.1016/j.humov.2013.10.007

Table 1
Limits of each degree of freedom (DOF) for the SAAM driving simulator.

DOF	Displacement	Velocity	Acceleration
Pitch	±22 deg	±30 deg/s	±500 deg/s^2
Roll	±21 deg	±30 deg/s	±500 deg/s^2
Yaw	±22 deg	±40 deg/s	±400 deg/s^2
Heave	±0.18 m	±0.30 m/s	±0.5 g
Surge	±0.25 m	±0.5 m/s	±0.6 g
Sway	±0.25 m	±0.5 m/s	±0.6 g

Table 2
Classical motion cueing algorithm parameters.

Symbol	Longitudinal	Lateral	Roll	Pitch	Yaw
2nd order LP cut-off frequency (Hz)			0.3	0.7	
2nd order LP damping factor			0.3	0.7	
1st order LP time constant (s)	0.1	0.1			0.1
2nd order HP cut-off frequency (Hz)	0.5	0.5			2
2nd order HP damping factor	1	1			1
1st order HP time constant (s)	2	2			2

heading reset at a single instant in time. This had the advantage that all co-ordinate systems could be aligned with a single action (Aykent et al., 2013; XSens Technologies BV 15, 2010). The details about the XSens motion tracking sensor are given in (Aykent et al., 2013; XSens Technologies BV 15, 2010).a_{x_head} and $a_{x,sensed}$; a_{y_head} and $a_{y,sensed}$ are equal to each other and they represent the measurements at the participants' ears as in Fig. 3 depending on the superposition principle of the translational and the rotational motions based on Eqs. (1) and (2).

2.3. Vehicle level data acquisition

Vehicle level data registered by SCANeRstudio software can be splitted as; command data (steering wheel angle, gas, brake pedal input, etc.), motion platform level (translational and angular accelerations of the hexapod platform), vehicle level data (vehicle dynamics, engine, etc.), frequential analysis of the motion platform and vehicle levels (by using FFT (Fast Fourier Transform)) (Aykent et al., 2013).

2.4. Postural level data acquisition

Postural stability of the subjects were identified by using a stabilotest of Technoconcept (Fig. 4). The measurements were performed as eyes open, after the driving sessions at the simulator. The data acquisition was done for 30 s at 40 Hz. Fast Fourier Transform (FFT) of the longitudinal and lateral displacements of the centre of pressure (CP) for the participants' bodies were registered at static and dynamic platform conditions. The participants were asked to get on the postural stability platform just after the completion of each driving session.

2.5. Protocol

Two conditions were driven by the driver-subjects for the specific scenario on the simulator real-time. The experiment protocol involved two phases of the driving situations as static and dynamic platform conditions on a country road scenario (Fig. 5).

Fig. 5 also depicts the *X*–*Y* trajectory and the vehicle velocity profile which were realized in the experiment phases. The whole experimental phase was completed with a constant velocity of 60 km/h in 120 s.

Please cite this article in press as: Aykent, B., et al. The role of motion platform on postural instability and head vibration exposure at driving simulators. *Human Movement Science* (2013), http://dx.doi.org/10.1016/j.humov.2013.10.007

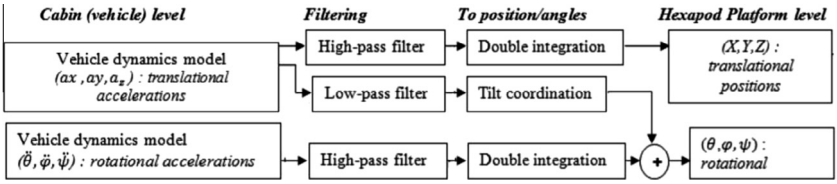

Fig. 2. Motion cueing algorithm.

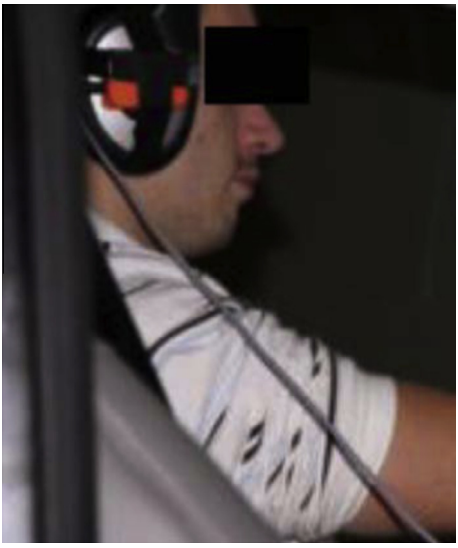

Fig. 3. Head level data acquisition during the experiments.

2.6. Subjects

The experimental procedure was done for static and dynamic platform cases. 47 subjects ($N = 47$, 35 males and 12 females) aged (mean: 31.32 years, SD: 8.05 years) and with driving licence experience (mean: 11.81 years, SD: 7.72 years) (SD: standard deviation) participated in experiments. 9 participants were carrying glasses (8 males, 1 female) and all the subjects were measured as with shoes worn.

3. Data analysis

The role of having a motion platform on postural instability and head level vibration exposures was discussed here for the sensed longitudinal and lateral dynamics regarding driving simulators.

In order to assess this, the head and vehicle level longitudinal and lateral accelerations (a_x, a_y) were collected by using a motion tracking sensor (Fig. 3) and SCANeRstudio software respectively.

Pearson's correlation was computed between the conditions of static and dynamic driving simulator situations in order to assess the optic-head inertial coupling. According to this; if the acceleration at vehicle level is negatively correlated to the acceleration at head level, it represents a less realistic driving simulation session. And if they are positively correlated to each other, it reveals a convergence to the reality.

Subjects were asked to complete a specific driving scenario under two types of operating conditions (static vs. dynamic platform) on the driving simulator. Each subject was tested once in each

Please cite this article in press as: Aykent, B., et al. The role of motion platform on postural instability and head vibration exposure at driving simulators. *Human Movement Science* (2013), http://dx.doi.org/10.1016/j.humov.2013.10.007

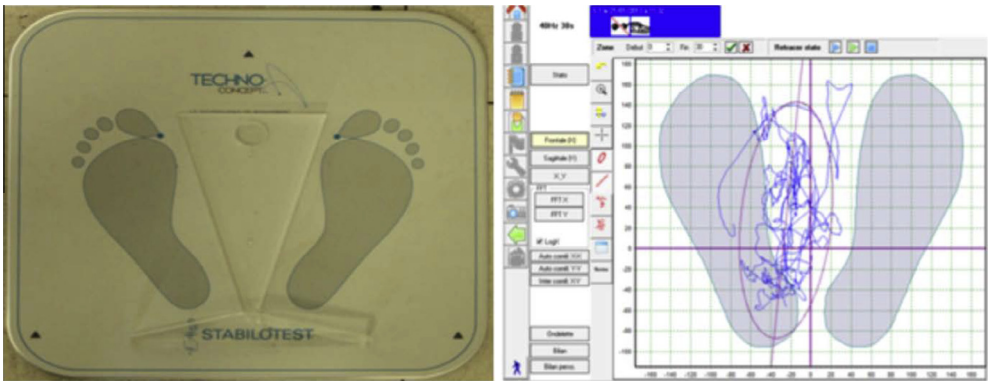

Fig. 4. Hardware and software tools for the postural instability measurement.

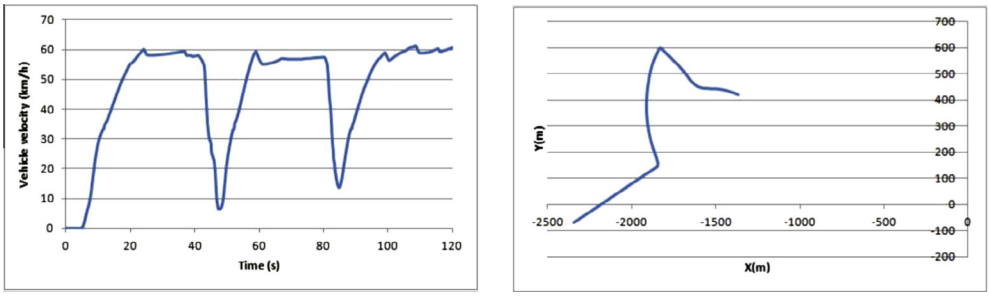

Fig. 5. Vehicle's velocity and *X*–*Y* trajectory during the experiments.

condition. Thus, it was a within-subjects variable for the two-tailed t tests and the two-tailed Mann-Whitney *U* tests.

Two-tailed *t* tests were assigned to compare the differences of the participants' body centre of pressure (CP) displacements, in terms of the influence of the motion platform, just after the each driving session.

Two-tailed Mann-Whitney *U* tests, which are non-parametric hypothesis tests, were benefited to assess the effect of motion platform on head level longitudinal and lateral vibration dose values (VDV) by using XLSTAT statistics software. In this article, head longitudinal and lateral VDVs refer to the head vibration exposures in longitudinal and lateral directions respectively (Eqs.(4) and (5)).

4. Results and discussion

In this section, the associations of longitudinal and lateral accelerations on the vehicle and the head levels (Figs. 6 and 7) and their level of significance were discussed as of having and not having the motion platform during the driving simulator operations.

Figs. 6 and 7 explained briefly the impact of the inertial stimulus (motion platform) as illustrating the mean value for all the subjects. The red curves illustrated the head level sensed longitudinal and lateral accelerations from the dynamic platform experiments, whereas the blue ones were depicting the head level longitudinal and lateral accelerations for the static platform conditions which could also be computed from (Eqs. (1) and (2)respectively). The black curves were illustrating the longitudinal and lateral accelerations of the vehicle centre of pressure and it was same for the both cases.

Please cite this article in press as: Aykent, B., et al. The role of motion platform on postural instability and head vibration exposure at driving simulators. *Human Movement Science* (2013), http://dx.doi.org/10.1016/j.humov.2013.10.007

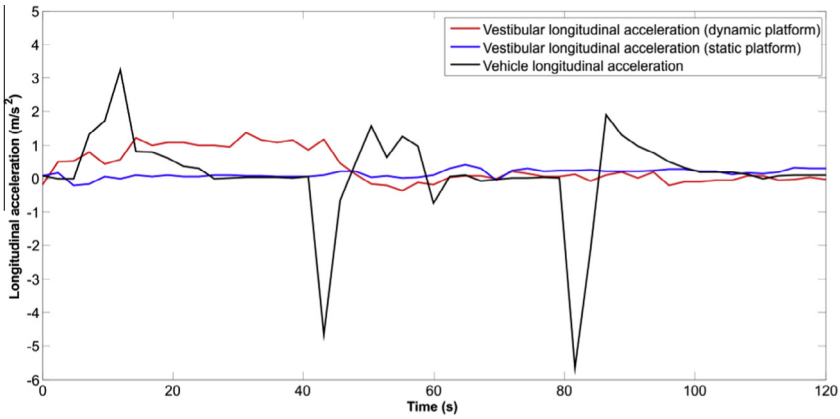

Fig. 6. The mean of vehicle-head level longitudinal accelerations at static and dynamic conditions.

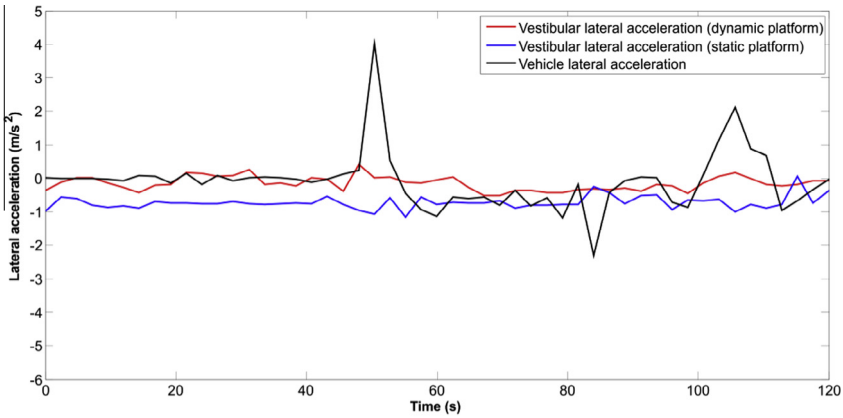

Fig. 7. The mean of vehicle-head level lateral accelerations at static and dynamic conditions.

Depending on these graphs, the visual and head longitudinal accelerations indicated a negative non-significant correlation ($r = -.203$, $p = .154 > .05$), whereas the optic-head inertial lateral accelerations revealed a negative significant correlation ($r = -.376$, $p = .007 < .05$) for the static platform.

For the dynamic platform case, the visual and head longitudinal accelerations depicted a very small neglectable negative non-significant correlation ($r = -.066$, $p = .643 > .05$), whereas the optic-head inertial lateral accelerations revealed a positive significant correlation ($r = .418$, $p = .002 < .05$).

The optic-head inertial lateral accelerations' gap reduction during the first curvature turn (45–50 s) was sourcing from the onset cueing in favor of the classical motion drive algorithm (dynamic platform) in general. The better fit of the optic-head inertial lateral acceleration signals on the steering maneuver just after the second curvature turn (105–110 s) was by the agency of onset cueing washout. The close optic-head inertial lateral acceleration fit in the end sections (110–120 s) (Fig. 7) arose by the tilt coordination and the time delays which were integrated in real-time (as seen in Fig. 2, Tables 1 and 2) for the dynamic platform condition whereas there was a mismatch of optic-head inertial cues for the static platform case.

Fig. 8 showed that post-exposure effect of hexapod motion platform on the longitudinal postural instability of the drivers. Regarding this figure, the maximum longitudinal displacement of the bodies CP yielded 6.489 mm higher in the static situation compared to the dynamic condition.

Please cite this article in press as: Aykent, B., et al. The role of motion platform on postural instability and head vibration exposure at driving simulators. *Human Movement Science* (2013), http://dx.doi.org/10.1016/j.humov.2013.10.007

The mean and the standard deviation (SD) values were given in Table 3. According to this table, the longitudinal displacement (X_{CP}) of the subject's body for the dynamic case revealed as 0.508 ± 1.594 mm, whereas it was 0.403 ± 1.673 mm at the static platform condition. In the table below, "dyn" refers to dynamic and "sta" refers to the static platform.

A two-tailed t test proved that there was a significant effect of having a motion platform on longitudinal postural displacements of the drivers. The X_{CP} for the dynamic case indicated a significant higher value rather than the static situation ($t(47)$, $p < .0001$; Fig. 9). As the computed p-value ($p < .0001$) is lower than the significance level alpha = .05, one should reject the null hypothesis H0, and accept the alternative hypothesis Ha after applying the two-tailed t test to check the difference significancy between the static and dynamic situations of the X_{CP} values of the drivers where the tested hypotheses were given below:

H0. The difference of location between the samples from the static and the dynamic cases is equal to 0.

Ha. The difference of location between the samples from the static and the dynamic cases is different from 0.

The graphic below (Fig. 10) showed that post-exposure effect of hexapod motion platform on the lateral postural instability of the drivers. Regarding this figure, the maximum lateral displacement of the bodies CP yielded 5.583 mm higher in the static situation compared to the dynamic condition.

The mean and the standard deviation (SD) values were given in Table 4. According to this table, the lateral displacement (Y_{CP}) of the subject's body for the dynamic case resulted as 0.638 ± 2.078 mm, whereas it was 0.731 ± 2.365 mm at the static platform condition. In the table below, dyn refers to dynamic and sta refers to the static platform.

A two-tailed t test yielded that there was a significant effect of having a motion platform on lateral postural displacements of the drivers. The Y_{CP} for the static case indicated a significant higher value rather than the dynamic situation ($t(47)$, $p = .001 < .05$; Fig. 11).

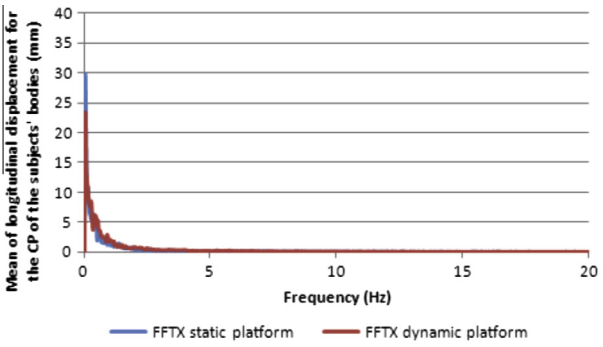

Fig. 8. The mean of FFT for the longitudinal displacement (X_{CP}) of the participants' bodies at static and dynamic platforms.

Table 3
Comparison of longitudinal displacements of participant bodies' CP for static and dynamic platforms.

Variable	Minimum	Maximum	Mean ± SD
X_{CP} of subject's body-dyn (mm)	0.000	23.034	0.508 ± 1.594
X_{CP} of subject's body-sta (mm)	0.000	29.523	0.403 ± 1.673

Please cite this article in press as: Aykent, B., et al. The role of motion platform on postural instability and head vibration exposure at driving simulators. *Human Movement Science* (2013), http://dx.doi.org/10.1016/j.humov.2013.10.007

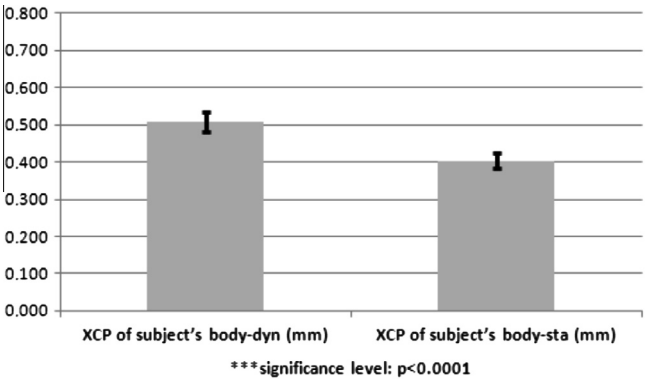

Fig. 9. Comparison of the longitudinal displacement (X_{CP}) of the participants' bodies at static and dynamic platforms: Error bars represent the confidence interval of 95%.

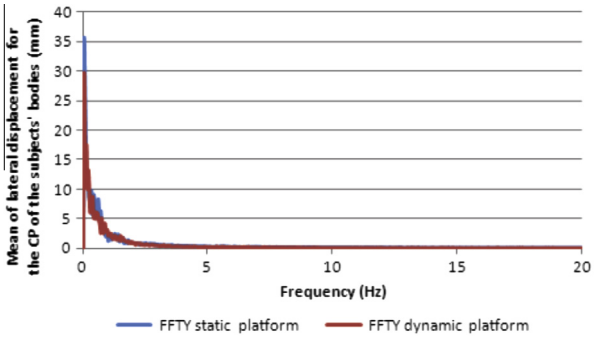

Fig. 10. The mean of FFT for the lateral displacement (Y_{CP}) of the participants' bodies at static and dynamic platforms.

Table 4
Comparison of lateral displacements of participant bodies' CP for static and dynamic platforms.

Variable	Minimum	Maximum	Mean ± SD
Y_{CP} of subject's body-dyn (mm)	0.000	29.259	0.638 ± 2.078
Y_{CP} of subject's body-sta (mm)	0.000	34.842	0.731 ± 2.365

Fig. 12 showed that the effect of hexapod motion platform on the head level longitudinal vibration exposures of the drivers. Regarding this figure, the maximum head level longitudinal VDV yielded 1.647 m $s^{-1.75}$ lower in the static platform compared to the dynamic condition.

The mean and the standard deviation (SD) values were given in Table 5. According to this table, the head level longitudinal vibration exposure (VDV_x) for the dynamic case resulted as 2.010 ± 0.571 m $s^{-1.75}$, whereas it was 0.421 ± 0.173 m $s^{-1.75}$ at the static platform condition. In the table below, "dyn" refers to dynamic and "sta" refers to the static platform.

A two-tailed Mann-Whitney *U* test indicated that there was a significant effect of having a motion platform on head level longitudinal vibration exposure (VDV_x). The VDV_x for the dynamic case indicated a significant higher value rather than the static situation ($U(47)$, $p < .0001$; Fig. 13). Since the computed *p*-value ($p < .0001$) is lower than the significance level alpha = 0.05, one should reject the null hypothesis H0, and accept the alternative hypothesis Ha after applying the two-tailed

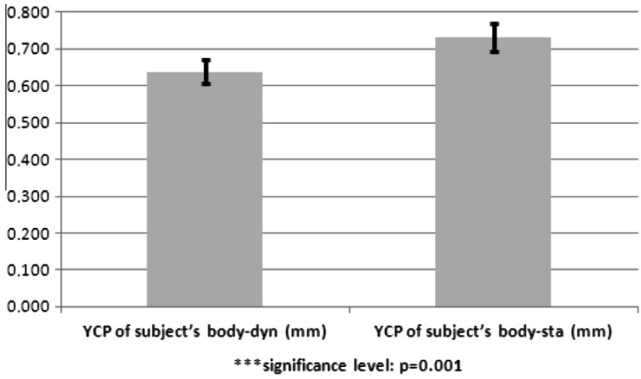

Fig. 11. The mean of head level longitudinal VDV at static and dynamic conditions.

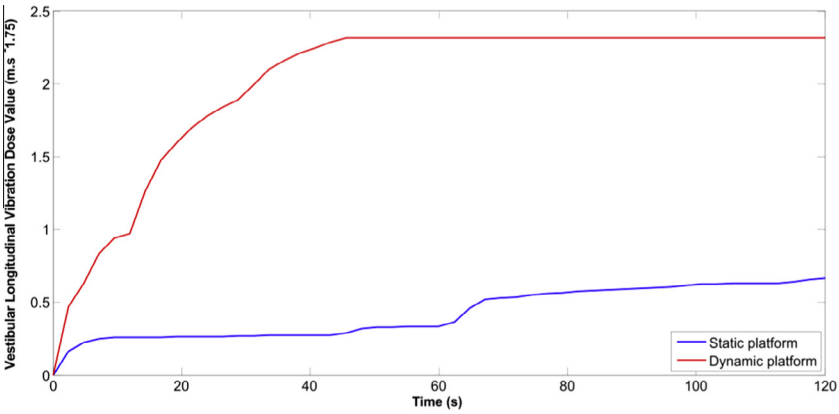

Fig. 12. Comparison of the lateral displacement (Y_{CP}) of the participants' bodies at static and dynamic platforms: Error bars represent the confidence interval of 95%.

Mann-Whitney *U* test to check the difference significancy between the static and dynamic situations of the head level sensed lateral VDVs where the tested hypotheses were given below:

H0. The difference of location between the samples from the static and the dynamic cases is equal to 0.

Ha. The difference of location between the samples from the static and the dynamic cases is different from 0.

Fig. 14 showed that the effect of hexapod motion platform on the head level lateral vibration exposures of the drivers. Regarding this figure, the maximum head level longitudinal VDV yielded 0.861 m $s^{-1.75}$ higher in the static platform compared to the dynamic condition.

Table 5
Comparison of head level longitudinal VDV for static and dynamic platforms.

Variable	Minimum	Maximum	Mean ± SD
VDV_x-dyn (m $s^{-1.75}$)	0.000	2.314	2.010 ± 0.571
VDV_x-sta (m $s^{-1.75}$)	0.000	0.667	0.421 ± 0.173

Please cite this article in press as: Aykent, B., et al. The role of motion platform on postural instability and head vibration exposure at driving simulators. *Human Movement Science* (2013), http://dx.doi.org/10.1016/j.humov.2013.10.007

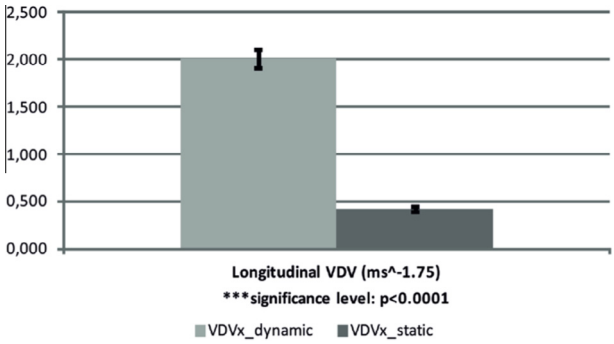

Fig. 13. Comparison of the head level longitudinal VDV at static and dynamic platforms: Error bars represent the confidence interval of 95%.

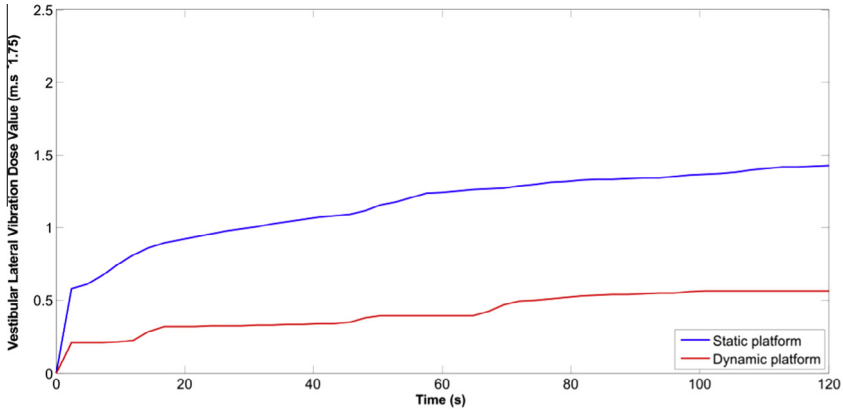

Fig. 14. The mean of head level lateral VDV at static and dynamic conditions.

Table 6
Comparison of head level lateral VDV for static and dynamic platforms.

Variable	Minimum	Maximum	Mean ± SD
VDV_y-dyn (m $s^{-1.75}$)	0.000	0.565	0.414 ± 0.132
VDV_y-sta (m $s^{-1.75}$)	0.000	1.426	1.139 ± 0.279

The mean and the standard deviation (SD) values were given in Table 6. According to this table, the head level lateral vibration exposure (VDV_y) for the dynamic case resulted as 0.414 ± 0.132 m $s^{-1.75}$, whereas it was 1.139 ± 0.279 m $s^{-1.75}$ at the static platform condition. In the table below, dyn refers to dynamic and sta refers to the static platform.

A two-tailed Mann-Whitney *U* test revealed that there was a significant effect of having a motion platform on vestibular level lateral vibration exposure (VDV_y). The VDV_y for the static case indicated a significant higher value rather than the dynamic situation ($U(47)$, $p < .0001$; Fig. 15).

Please cite this article in press as: Aykent, B., et al. The role of motion platform on postural instability and head vibration exposure at driving simulators. *Human Movement Science* (2013), http://dx.doi.org/10.1016/j.humov.2013.10.007

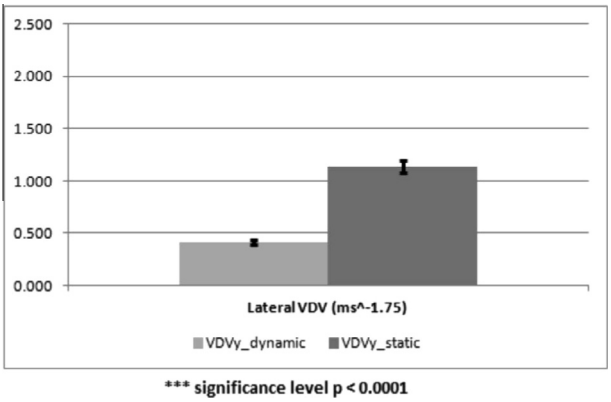

Fig. 15. Comparison of the head level lateral VDV at static and dynamic platforms: Error bars represent the confidence interval of 95%.

5. Conclusion

The influence of having motion platform on postural instability and head level vibration exposures on driving simulators was discussed in this paper. After having completed these experimental phases, it was yielded that the dynamic platform provided a closer lateral dynamics representation between real-time vehicle model (optic cues) and real-time head dynamics cue levels. It could be concluded that having dynamic platform represented a reconciling to real-world applications associated to lateral dynamics in terms of data acquisition and measurements.

It can be summed up concisely that the X_{CP} (longitudinal body centre of pressure displacements) for the dynamic case indicated a significant higher value rather than the static situation. The VDV_x (head level longitudinal vibration dose value) for the dynamic case indicated a significant higher value rather than the static situation.

It can also be deduced apparently from this study that the VDV_y (head level lateral vibration dose value) for the static case indicated a significant higher value rather than the dynamic situation. Furthermore, the Y_{CP} (lateral body centre of pressure displacements) for the static case indicated a significant higher value rather than the dynamic situation.

References

Abercromby, A. F., Amonette, W. E., Layne, C. S., et al (2007). Vibration exposure and biodynamic responses during whole-body vibration training. *Medicine and Science in Sports and Exercise, 39*(10), 1794.

Aykent, B., Paillot, D., Merienne, F., Kemeny, A. (2012). A LQR washout algorithm for a driving simulator equipped with a hexapod platform: The relationship of neuromuscular dynamics with the sensed illness rating. CONFERE, 5–6 July 2012, Venice, Italy.

Aykent, B., Merienne, F., Paillot, D., & Kemeny, A. (2013). Influence of inertial stimulus on visuo-vestibular cues conflict for lateral dynamics at driving simulators. *Journal of Ergonomics, 3*, 1–7.

Aykent, B., Paillot, D., Merienne, F., & Kemeny, A. (2012b). *The Influence of the feedback control of the hexapod platform of the SAAM dynamic driving simulator on neuromuscular dynamics of the drivers*. Paris, France: Driving Simulation Conference.

Benson, A., J., 1988. Motion sickness. In Medical aspects of harsh environments, Vol. 2. (pp. 1048–1083), United Kingdom.

Berthoz, A., Pavard, B., & Young, L. (1975). Perception of linear horizontal self-motion induced by peripheral vision (linearvection) basic characteristics and visual-vestibular interactions. *Experimental Brain Research, 23*, 471–489.

Bertin, R., & Berthoz, A. (2004). Visuo-vestibular interaction in the reconstruction of travelled trajectories. *Experimental Brain Research, 154*, 11–21.

Bonnet, C. T., Faugloire, E., Riley, M. A., Bardy, B. G., & Stoffregen, T. A. (2006). Motion sickness preceded by unstable displacements of the center of pressure. *Human Movement Science, 25*(6), 800–820.

Bremmer, F., Kubischik, M., Pekel, M., Lappe, M., & Hoffmann, K. P. (1999). Linear vestibular self-motion signals in monkey medial superior temporal area. *Annals of the New York Academy of Sciences, 871*, 272–281.

Curry, R., Artz, B., Cathey, L., Grant, P., & Greenberg, J. (2002). Kennedy ssq results: Fixed-vs motion-based FORD simulators. *Proceedings of DSC*, 289–300.

Please cite this article in press as: Aykent, B., et al. The role of motion platform on postural instability and head vibration exposure at driving simulators. *Human Movement Science* (2013), http://dx.doi.org/10.1016/j.humov.2013.10.007

Dichgans, J., & Brandt, T. (1973). Optokinetic motion sickness and pseudo-coriolis effects induced by moving visual stimuli. *Acta Oto-Laryngologica, 76*(1–6), 339–348.

Dizio, P., & Lackner, J. (1988). The effects of gravitoinertial force level and head movements on post-rotational nystagmus and illusory after-rotation. *Experimental Brain Research, 70*(3), 485–495.

DiZio, P., & Lackner, J. (1989). Perceived self-motion elicited by postrotary head tilts in a varying gravitoinertial force background. *Attention, Perception, & Psychophysics, 46*, 114–118.

Dong, X., Yoshida, K., & Stoffregen, T. A. (2011). Control of a virtual vehicle influences postural activity and motion sickness. *Journal of Experimental Psychology: Applied, 17*(2), 128.

Draper, M. (1998). *The adaptive effects of virtual interfaces: Vestibulo-ocular reflex and simulator sickness*. University of Washington.

Griffin, M. J. (2004). Minimum heath and safety requirements for workers exposed to handtransmitted vibration and whole-body vibration in the European Union; a review. *Occupational and Environmental Medicine*, 387–397.

Guedry, F. E. (1964). Visual control of habituation to complex vestibular stimulation in man. *Acta Oto-Laryngologica, 58*(1–6), 377–389.

Guedry, F. E., & Montague, E. K. (1961). Quantitative evaluation of the vestibular coriolis reaction. *Aerospace Medicine, 32*(6), 487.

Hettinger, L. (2002). Illusory self-motion in virtual environments. In Handbook of virtual environments Design implementation and applications, Lawrence Erlbaum.

Hettinger, L., Berbaum, K., Kennedy, R., Dunlap, W., & Nolan, M. (1990). Vection and simulator sickness. *Military Psychology, 2*, 171–181.

Hettinger, L., & Riccio, G. (1992). Virtually induced motion sickness in virtual environments. *Presence: Teleoperators and Virtual Environments, 1*(3), 306–310.

ISO 2631-1, 1997. Mechanical vibration and shock: Evaluation of human exposure to whole-body vibration. Part 1, general requirements.

Kennedy, R. S., Berbaum, K. S., Lilienthal, M. G., Dunlap, W.P., Mulligan, B. E. (1987). Guidelines for alleviation of simulator sickness symptomatology. Tech. rep., DTIC Document.

Kolasinski, E. (1995). Simulator sickness in virtual environments. DTIC Document.

Lepecq, J., De Waele, C., Mertz-Josse, S., Teyssèdre, C., Huy, P., Baudonnière, P., et al (2006). Galvanic vestibular stimulation modifies vection paths in healthy subjects. *Journal of Neurophysiology, 95*, 3199–3207.

McCauley, M., & Sharkey, T. (1992). Cybersickness- perception of self-motion in virtual environments. *Presence: Teleoperators and Virtual Environments, 1*, 311–318.

Reason, J., & Brand, J. (1975). *Motion sickness*. Academic Press.

Riccio, G., & Stoffregen, T. (1991). An ecological theory of motion sickness and postural instability. *Ecological Psychology, 3*(3), 195–240.

Smart, L. J., Stoffregen, T. A., & Bardy, B. G. (2002). Visually induced motion sickness predicted by postural instability. *Human Factors: The Journal of the Human Factors and Ergonomics Society, 44*(3), 451–465.

Stratulat, A., Roussarie, V., Vercher, J., & Bourdin, C. (2010). Does tilt/translation ratio affect perception of deceleration in driving simulators? *Journal of Vestibular Research, 21*, 127–139.

Watson, G. (2000). A synthesis of simulator sickness studies conducted in a high-fidelity driving simulator. *Proceedings of Driving Simulation Conference*, 69–78.

XSens Technologies BV 15, 2010. MTi and MTx user manual and technical documentation. Document MT0100P, Revision O.

Please cite this article in press as: Aykent, B., et al. The role of motion platform on postural instability and head vibration exposure at driving simulators. *Human Movement Science* (2013), http://dx.doi.org/10.1016/j.humov.2013.10.007